First ^{17}O NMR Observation of Coordinated Water on Both Isomers of $[Eu(DOTAM)(H_2O)]^{3+}$: A Direct Access to Water Exchange and its Role in the Isomerization[1]

Frank A. Dunand,[†] Silvio Aime,*[,‡] and André E. Merbach*[,†]

Contribution from the Institut de Chimie Minérale et Analytique, Université de Lausanne, CH-1015 Lausanne, Switzerland, and Dipartimento di Chimica I.F.M., Universita di Torino, I-10125 Torino, Italy

Received September 3, 1999. Revised Manuscript Received December 1, 1999

Abstract: A complete mechanistic study of the solution dynamics of $[Eu(DOTAM)(H_2O)]^{3+}$ is performed through ^1H and ^{17}O NMR variable pressure and temperature studies. An unambiguous understanding of the water exchange was possible thanks to the first ^{17}O NMR observation of the bound water signal on both the M- and m-isomers (M: $k_M^{250} = 0.113 \pm 0.013 \times 10^3$ s^{-1}, $k_M^{298} = 8.3 \pm 0.3 \times 10^3$ s^{-1}, $\Delta H^{\ddagger} = 53.1 \pm 2$ kJ mol^{-1}, $\Delta S^{\ddagger} = +8.4 \pm 5$ J K^{-1} mol^{-1}, $\Delta V^{\ddagger} = +4.9 \pm 1$ cm^3 mol^{-1}; m: $k_M^{250} = 8.9 \pm 0.6$ s^{-1}, $k_M^{298} = 327 \pm 60 \times 10^3$ s^{-1}, $\Delta H^{\ddagger} = 44.2 \pm 2$ kJ mol^{-1}, $\Delta S^{\ddagger} = +8.8 \pm 7$ J K^{-1}mol^{-1}). The water exchange on m is about 50 times faster than on M, and even though the equilibrium constant $K = [M]/[m]$ equals 4.5, the contribution of m to the overall exchange rate is 90%. These results can be transferred to an aqueous solution since they agree with the overall exchange rate obtained by ^{17}O NMR for an aqueous solution of $[Gd(DOTAM)(H_2O)]^{3+}$. 2D-EXSY and variable temperature and pressure ^1H NMR experiments reveal that the interconversion between the M and m isomers happens mainly through a rotation of the amide arms in an interchange activated mechanism. (Interconversion rates measured by magnetization transfer: M → m: $k_a^{250} = 60 \pm 10$ s^{-1}; m → M: $k_a^{250} = 260 \pm 50$ s^{-1}. Activation volumes: M → m: $\Delta V^{\ddagger} = -0.5 \pm 0.3$ cm^3 mol^{-1}, m → M: $\Delta V^{\ddagger} = -0.5 \pm 0.7$ cm^3 mol^{-1} and reaction volume $\Delta V^{\circ} = 0 \pm 1$ cm^3 mol^{-1}). In light of a simultaneous fitting of the water exchange and interconversion NMR data (M → m: $\Delta H^{\ddagger} = 39.1 \pm 1.9$ kJ mol^{-1}, $\Delta S^{\ddagger} = -52.1 \pm 7.4$ J K^{-1}mol^{-1}, $k^{250} = 68 \pm 5$ s^{-1}), as well as an interpretation of the activation and reaction volumes, we deduce a correlation between the two processes. A nonhydrated complex is proposed as a common intermediate for both the water exchange and the arm rotation processes, but only one M → m interconversion happens while two to three water exchanges take place.

Introduction

Nowadays, gadolinium polyaminocarboxylate complexes are commonly used as MRI contrast agents.[2,3] Among the macrocyclic systems, the DOTA ligand was early recognized as an excellent candidate for this kind of applications due to the outstanding thermodynamic stability of its complexes with Ln(III) ions (DOTA = 1,4,7,10-tetraaza-1,4,7,10-tetrakis(carboxymethyl)cyclododecane).

$[Gd(DOTA)]^-$ was the second complex entered into clinical practice (Dotarem, Guerbet, France) soon followed by the strictly related [Gd(HP-DO3A)] (Prohance, Bracco, Italy). Both complexes function effectively as general purpose extracellular agents, and the DOTA skeleton represents the model for the development of novel contrast agents characterized either by a higher relaxivity or an improved specificity. One of the important points to be understood in order to design new potential Gd-based MRI contrast agents is the relationship between the structure, the rate, and the mechanism of the water exchange, as this is one of the limiting factors next to the tumbling time and the electronic relaxation.[4,5]

It is now well-known that $[Ln(DOTA)(H_2O)]^-$ complexes exist in two diastereoisomeric forms, m and M, that differ by the layout of their acetate arms: the M-isomer has an antiprismatic geometry whereas the m isomer has a twisted antiprismatic geometry.[6] Basically the two structures display a different orientation of the two square planes formed by the four nitrogens and the four oxygens, making an angle of ca. 40° in M-type structures whereas it is reversed and reduced to ca. 20° in the m-type derivatives. Such arrangements appear common to all chelates containing DOTA-like ligands such as the DOTA-tetramide considered in this work. In the case of $[Ln(DOTA)(H_2O)]^-$ complexes, solid-state X-ray m-type structures have been observed for La and Ce[7] whereas M-type structures have been reported for Ln(III) = Eu, Gd, Dy, Ho, Lu, and Y.[8−11]

* Address correspondence to André A. Merbach, Institut de Chimie Minérale et Analytique, Université de Lausanne, CH-1015 Lausanne, Switzerland. E-mail: andre.merbach@icma.unil.ch.

† Université de Lausanne.

‡ Universita di Torino.

(1) Part 91 of the series *High-Pressure NMR Kinetics.* For part 90, see Churlaud, R.; Frey, U.; Metz, F.; Merbach, A. E. Submitted for publication.

(2) Koenig, S. H.; Brown, R. D. I. In *NMR in Physiology and Biomedicine*; Academic Press: New York, 1994; pp 57−73.

(3) Lauffer, R. B. *Chem. Rev.* **1987**, *87*, 901−927. (b) Caravan, P.; Ellison, J. J.; McMurry, T. J.; Lauffer, R. B. *Chem. Rev.* **1999**, *99*, 2293−2352.

(4) Powell, D. H.; Favre, M.; Graeppi, N.; Ni Dhubhghaill, O. M.; Pubanz, D.; Merbach, A. E. *J. Alloys Compd.* **1995**, *225*, 246−252.

(5) Powell, D. H.; Ni Dhubhghaill, O. M.; Pubanz, D.; Lebedev, Y.; Schlaepfer, W.; Merbach, A. E. *J. Am. Chem. Soc.* **1996**, *118*, 9333−9346.

(6) Aime, S.; Botta, M.; Ermondi, G. *Inorg. Chem.* **1992**, *31*, 4291−4299.

(7) Bombieri, G. To be published.

10.1021/ja993204s CCC: $19.00
Published on Web 02/05/2000

Scheme 1. Schematic Structure of the Two Diasteroisomers of the Complex $[Eu(DOTAM)(H_2O)]^{3+}$. The Coordinated Water Molecule, Located above the Plan of the Four Oxygens, Has Been Omitted for Clarity

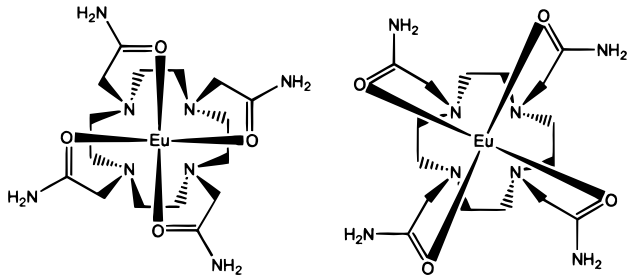

Analogously, for DOTA-tetramide Ln(III) complexes an m-type structure has been found in the case of $[Eu(DOTAM)(H_2O)]^{3+}$ [12] whereas the Dy complexes with the ligands where one or both amide protons have been substituted by methyl groups gave X-ray structures corresponding to M-type ones (DOTAM = 1,4,7,10-tetrakis(carbamoylmethyl)-1,4,7,10-tetraazacyclododecane).[13]

The bound water signal of $[Ln(DOTA)(H_2O)]^-$ complexes has never been observed due to the fast exchange ($k_{ex}^{298} = 4.1 \times 10^6$ s^{-1}, for Gd(III), which is an average value for the two isomers weighted by their respective mole fraction).[5] Recently it has been shown that the exchange can be slowed by replacing the carboxylates by *N*-methyl-carboxamide groups.[14] Empirically the replacement of one binding carboxylate group by an amide group slows down the exchange by a factor of 3 to 4,[15] i.e., the average rate for a tetraamide-DOTA complex should be in the order of $2-5 \times 10^4$ s^{-1}. Actually an exchange rate of 5.2×10^4 s^{-1} has been determined for $[Gd(DOTAM)(H_2O)]^{3+}$ by ^{17}O measurements.[13] Furthermore, on the basis of the ^1H NMR spectra of the $[Eu(DOTAM)(H_2O)]^{3+}$ complex (which exists in solution in the two isomeric forms M and m (Scheme 1)), the water exchange was found to be much faster on m than on M.[16]

The aim of the present work on $[Eu(DOTAM)(H_2O)]^{3+}$ is to understand the mechanism of the water exchange from variable temperature and pressure ^1H and ^{17}O NMR data. This was made possible by the first ^{17}O NMR observation of both bound water signals. Simultaneously, we studied the mechanism of the M $\rightleftarrows$ m interconversion by magnetization transfer experiments, as well as by variable temperature and pressure ^1H NMR. Finally, a correlation between the two processes will be presented and discussed.

(8) Aime, S.; Barge, A.; Botta, M.; Fasano, M.; Ayala, J. D.; Bombieri, G. *Inorg. Chim. Acta* **1996**, *246*, 423−429.
(9) Parker, D.; Pulukkody, K.; Smith, F. C.; Batsanov, A.; Howard, J. A. K. *J. Chem. Soc., Dalton Trans.* **1994**, 689−693.
(10) Benetollo, F.; Bombieri, G.; Aime, S.; Botta, M. *Acta Crystallogr. Sect. C Cryst. Struct. Commun.* **1999**, *55*, 353−356.
(11) Dubost, J. P.; Leger, J. M.; Langlois, M. H.; Meyer, D.; Schaefer, M. *C. R. Acad. Sci. Paris* **1991**, *312*, 349−354.
(12) Amin, S.; Morrow, J. R.; Lake, C. H.; Churchill, M. R. *Ang. Chem., Int. Ed. Engl.* **1994**, *33*, 773−775.
(13) Aime, S.; Barge, A.; Bruce, J. I.; Botta, M.; Howard, J. A. K.; Moloney, J. M.; Parker, D.; De Sousa, A. S.; Woods, M. *J. Am. Chem. Soc.* **1999**, *121*, 5762−5771.
(14) Aime, S.; Barge, A.; Botta, M.; Parker, D.; De Sousa, A. S. *J. Am. Chem. Soc.* **1997**, *119*, 4767−4768.
(15) Toth, E.; Burai, L.; Brucher, E.; Merbach, A. E. *J. Chem. Soc., Dalton Trans.* **1997**, 1587−1594.
(16) Aime, S.; Barge, A.; Botta, M.; De Sousa, A. S.; Parker, D. *Ang. Chem., Int. Ed.* **1998**, *37*, 2673−2675.
(17) Ammann, C.; Meier, P.; Merbach, A. E. *J. Magn. Res.* **1982**, *46*, 319−321.

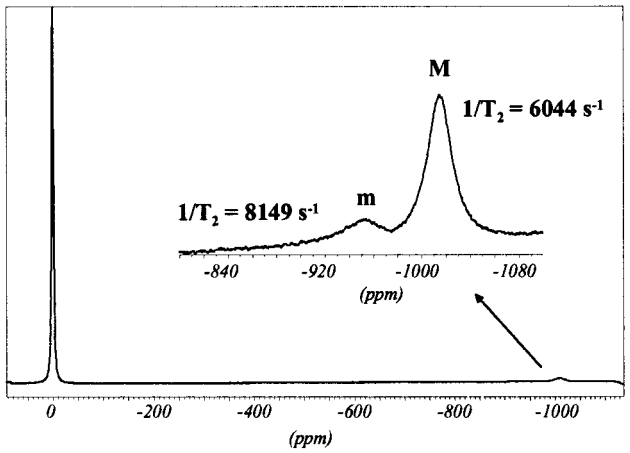

Figure 1. ^{17}O NMR spectrum (14.1 T) of $[Eu(DOTAM)(H_2O)]^{3+}$ ([Eu] = 29.3 mM, bound water/free water = 0.067) in CD_3CN at 235.2 K. The free water signal is taken as chemical shift reference.

Experimental Section

Sample Preparation. The ligand and the complex were prepared as previously described.[12,16] The solutions were prepared by dissolution of the solid complex $[Eu(DOTAM)(H_2O)](SO_3CF_3)_3$ in CD_3CN and H_2O with a drop of TMS as an internal reference. The Eu(III) concentration varies from 8 to 40 mM and the water content from 0.4 to 2%. For ^{17}O NMR measurements we used 40% ^{17}O-enriched proton normalized water (Yeda Co. LTD, Israel).

Variable Temperature NMR. The ^1H NMR and ^{17}O NMR spectra have been measured on Bruker ARX-400 and DPX-400 spectrometers. The temperature was stabilized by Bruker VT-2000 and BVT-3000 temperature control units and checked by a substitution method.[17]

Variable Pressure NMR. The ^1H and ^{17}O NMR measurements were performed using a narrow-bore 5 mm home-built high-pressure probehead on a ARX-400 Bruker spectrometer. A ^1H specific and a BBO probehead were used for the ^1H and ^{17}O experiments, respectively.[18] The pressure was produced using a manual pump, and $C_2Br_2F_4$ was used as pressurization liquid. The temperature was stabilized using industrial alcohol in a Huber cryothermostat HS 80 and checked with a Pt probe (Pt-100 Ω) connected to a calibrated digital Data Tracker 130 (Data Oricess Instrument).

Data Treatment. The NMR signals are fitted by a Lorentzian function with the program NMRICMA 2.5 for MATLAB developed by L. Helm in Lausanne. The half-width of the ^1H NMR lines are corrected by subtracting the half-width of the TMS line (inhomogeneity, line broadening); in the ^{17}O NMR measurements, the inhomogeneity effect can be neglected. The integrals are calculated by multiplying the fitted half-width by the height of the lines. The simultaneous fitting of the data to obtain the kinetic and thermodynamic parameters is performed by the program Scientist for Windows by Micromath, version 2.0.

Results and Discussion

Water Exchange. We first repeated and corrected the variable temperature ^1H NMR measurements reported in the preliminary publication.[16] Under our experimental conditions ($c_{Eu(DOTAM)} = 8-40$ mM, 0.4−2% H_2O, in CD_3CN or D_2O), the transverse relaxation rates of the bound water signals are independent of the complex concentration and of the solvent composition, thus the kinetic results should also apply to aqueous solutions. As expected, the line width of the free water signal depends on the molar fraction of the bound water, hence on the composition of the solution. For the first time we were also able to observe the ^{17}O NMR bound water signals (Figure 1), thus to measure their temperature dependence which allows

(18) Cusanelli, A.; Nicula-Dadci, L.; Frey, U.; Merbach, A. E. *Inorg. Chem.* **1997**, *36*, 2211−2217.

Table 1. Water Exchange Parameters Obtained from the Simultaneous and Separate Fitting of the ^{1}H and ^{17}O NMR Transverse Relaxation Rates of the Bound Water Signals (The underlined parameters were fixed for the fitting)

	separate ^{1}H and ^{17}O fits			simultaneous ^{1}H and ^{17}O fits [a]			
	M-isomer			M-isomer		m-isomer [b]	
	^{1}H	^{17}O	m-isomer:[b] ^{1}H	^{1}H	^{17}O	^{1}H	^{17}O
$k_{ex}^{250}/10^3$ s^{-1}	0.090 ± 0.008	0.112 ± 0.052	10.2 ± 1	0.113 ± 0.013		8.9 ± 0.6	
$k_{ex}^{298}/10^3$ s^{-1}	9.4 ± 0.2	7.4 ± 0.6	474 ± 130	8.3 ± 0.3		327 ± 60	
$\Delta H^{\ddagger}$/kJ mol^{-1}	57.5 ± 1	51.6 ± 5	47.2 ± 3	53.1 ± 2		44.2 ± 2	
$\Delta S^{\ddagger}$/J K^{-1} mol^{-1}	+24.1 ± 4	+2.4 ± 18	22 ± 11	+8.4 ± 5		8.8 ± 7	
$(1/T_{2B})^{298}$/s^{-1}	154.8 ± 17	1313 ± 264	100	134.5 ± 26	1186 ± 133	100	1335 ± 71
	122.6 ± 14	1304 ± 264		106.0 ± 21	1172 ± 140		
	164.7 ± 16			145.3 ± 24			
E_a/kJ mol^{-1}	9.3 ± 1	13.8 ± 2	10.3	10.3 ± 1	14.8 ± 1	10.3	14.8

[a] The bound water lifetimes ($\tau^{298} = 1/k_{ex}^{298}$) were reported as 18.8 μs (m-isomer) and 4.16 ms (M-isomer) in ref 16, but are now corrected to 3.06 μs (m-isomer) and 0.12 ms (M-isomer). This important correction of the preliminary values of rate constants (residence times) and activation parameters is due to previous errors in the data analysis and temperature measurements. [b] For the m-isomer the small observable temperature range (Figure 2) did not allow a separate fit of the ^{17}O data, but they could be included in a simultaneous treatment with the ^{1}H data.

the unambiguous determination of the water exchange parameters on the two isomers of $[Eu(DOTAM)(H_2O)]^{3+}$.

At the temperatures where the bound water signals are observable, the slow exchange approximation (eq 1) applies.

$$\pi W_{1/2}^{B} = \frac{1}{T_{2B}^{meas}} = \frac{1}{T_{2B}} + \frac{1}{\tau_B} \quad (1)$$

$W_{1/2}^{B}$ is the measured half width of the bound water signal, $1/T_{2B}$ is the transverse relaxation rate in the absence of exchange and τ_B is the residence time of the water molecule in the first coordination sphere. The temperature dependence of the water exchange rate k_{ex} ($= 1/\tau_B$) can be described by the Arrhenius equation (eq 2), where the symbols have their usual meaning.

$$\frac{1}{\tau_B} = k_{ex} = k_{ex}^{298}\frac{T}{298.15}\cdot\exp\left(\frac{\Delta H^{\ddagger}}{R}\left(\frac{1000}{298.15} - \frac{1000}{T}\right)\right) \quad (2)$$

$1/T_{2B}$ is assumed to follow an exponential law (eq 3) incorporating different contributions: dipolar and contact for proton and mainly quadrupolar for oxygen-17.

$$\frac{1}{T_{2B}} = \left(\frac{1}{T_{2B}}\right)^{298}\exp\left(\frac{E_a}{R}\left(\frac{1000}{T} - \frac{1000}{298.15}\right)\right) \quad (3)$$

The bound water line widths have been fitted to eqs 1−3 to yield the kinetic parameters reported in Table 1.

The ^{1}H and ^{17}O NMR variable temperature experiments were performed between 212 and 312 K. The data for both isomers are always analyzed separately. Furthermore, for each isomer the data were first fitted separately for both ^{1}H and ^{17}O nuclei and gave very similar exchange rates and activation enthalpies (see Supporting Information, Figure S1 and Table 1); hence, the proton exchange is due to the exchange of an entire water molecule. Therefore, ultimately both ^{1}H and ^{17}O NMR data were fitted simultaneously (Figure 2) to yield the final kinetic parameters reported in Table 1. The water exchange on the m-isomer is approximately 50 times faster than on the M-isomer (slightly temperature dependent due to a small difference in the activation enthalpies). Thanks to the observation of both ^{1}H and ^{17}O NMR bound water signals, and a larger temperature range, the accuracy of the kinetic parameters could be corrected with respect to the preliminary communication.[16]

In a general case, the bound water signals cannot be observed in solutions of paramagnetic complexes, and the temperature dependence of the free water signal is analyzed, using the Swift and Connick approach,[19] to obtain an average water exchange rate. Here we can take advantage of the bound water data to do the opposite and simulate the line width of the free water. We make the assumption that the broadening of the free water signal is due to the sum of the contributions of the exchange with both M- and m-isomers separately. Despite the fact that the bound water mole fraction (>5%) is beyond the Swift and Connick approximation limits (<5%), the simulated curves fit reasonably well the free water experimental data (see Supporting Information Figure S2).

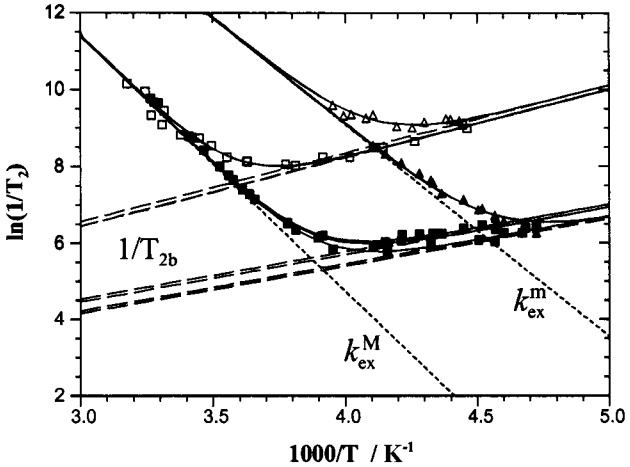

Figure 2. Simultaneous fit of the water exchange from ^{1}H (filled symbols) and ^{17}O (unfilled symbols) NMR data. The squares stand for the M-isomer and the triangles for the m-isomer. The solid, dotted, and dashed lines stand for the fitted transverse relaxation rates, the exchange contributions, and the transverse relaxation rates without exchange, respectively.

Considering the empirical rule that each replacement of a carboxylate in $[Gd(DOTA)(H_2O)]^{-}$ by an amide slows down the water exchange by a factor of 3 to 4,[15] we expect a weighted overall water exchange rate at 298 K of $2-5 \times 10^4$ s^{-1} for $[Eu(DOTAM)(H_2O)]^{3+}$. This overall water exchange rate can be calculated by a weighted addition of the contribution of both isomers (eq 4), where P_M and P_m are the mole fraction of the M- and m-isomer, respectively.

$$k_{ex}^{298} = P_M k_M^{298} + P_m k_m^{298} \quad (4)$$

If we consider an equilibrium constant $K = [M]/[m] = 4.5$ (vide infra) and the individual rates at 298 K reported in Table 1, we obtain a value of 7×10^4 s^{-1}. It agrees well with the

(19) Swift, T. J.; Connick, R. E. *J. Chem. Phys.* **1962**, *37*, *2*, 307−320.

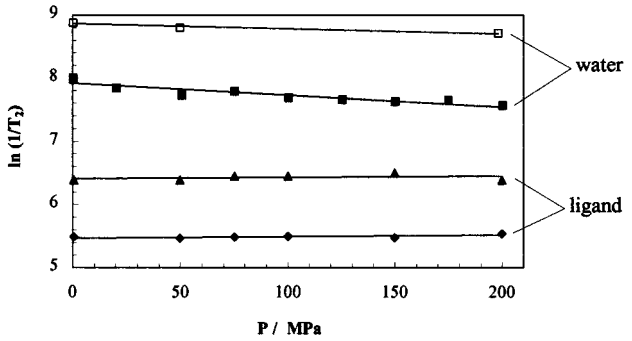

Figure 3. Pressure dependence of the NMR transverse relaxation rates. ◆ M_{eq2} proton at 256 K, ▲ m_{eq2} proton at 256 K, ■ bound water proton of M at 281 K, □ bound water ^{17}O of M at 293 K.

experimental value for the Gd(III) complex (5.2×10^4 s^{-1}), since the exchange must be slightly faster on the larger Eu(III) cation for a dissociatively activated process. These results are a further indication that our rates measured in acetonitrile can be generalized to an aqueous solution. Note that the estimated value was calculated on the basis of $[Gd(DOTA)(H_2O)]^-$ where $K > 4.5$.[20] Despite the fact that the m-isomer represents only about 20% of the total complex concentration, its contribution to the overall exchange rate is 90%.

At a given temperature, the water exchange rate depends on pressure following eq 5, where $\Delta V^{\ddagger}$ is the activation volume of the water exchange reaction and $k_{ex,0}$ the exchange rate at zero pressure.

$$k_{ex} = k_{ex,0} \exp\left(\frac{-\Delta V^{\ddagger}}{RT} P\right) \qquad (5)$$

The measured line width is related to k_{ex} by eq 1. The effect of pressure on the transverse relaxation rate in the absence of exchange ($1/T_{2B}$) can be neglected: first because the overall contribution of $1/T_{2B}$, calculated from the parameters obtained in the variable temperature study (eq 3), is <10% and <20% for the ^1H NMR measurements at 281.4 K and the ^{17}O NMR measurements at 292.8 K, respectively; second because the pressure dependence of $1/T_{2B}$ itself is known to be small.[21]

The line width of the bound water signal of the M-isomer was measured at different pressures from 0.3 to 200 MPa. The evolution of $\ln(1/T_2^{meas})$ of the proton signal upon pressure changes is shown in Figure 3. The activation volume was calculated from the ^1H NMR data ($\Delta V^{\ddagger} = 4.9 \pm 1$ cm^3 mol^{-1}) and is confirmed by ^{17}O NMR data ($\Delta V^{\ddagger} = 2.4 \pm 1$ cm^3 mol^{-1}, 3 pressures). The activation volume is clearly positive, suggesting a dissociative activation mode for the water exchange on the M-isomer. By analogy to Gd(III)-DOTA derivative complexes ($[Gd(DOTA)]^-$: $\Delta V^{\ddagger} = +10.5$ cm^3 mol^{-1}),[5] we can suggest a dissociative water exchange mechanism for $[Eu(DOTAM)(H_2O)]^{3+}$ considering that the small measured activation volume can be explained by a contraction of the coordination sphere in a the nonhydrated intermediate.

M ⇄ m Interconversion. Two sources of helicity are present in $[Eu(DOTAM)(H_2O)]^{3+}$ as in DOTA-like complexes.[20] One is due to the four five-membered rings formed by the binding of the amide arms to Eu(III), whose absolute configuration is described by Δ or Λ. The second is due to the four five-membered rings formed by the binding of the cyclen to Eu(III); its absolute configuration is described by δδδδ and λλλλ.

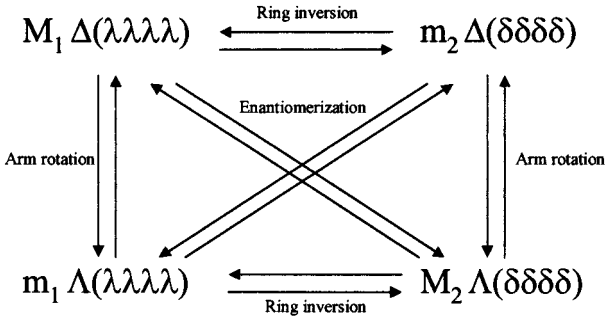

Figure 4. Isomerization processes involved in the equilibrium of $[Eu(DOTAM)(H_2O)]^{3+}$ in solution. Δ/Λ correspond to the absolute configuration of the amide arms and δδδδ/λλλλ to the absolute configuration of the four ethylenediamine groups that form the cycle.

Hence two different processes can lead to an M ⇄ m interconversion: (1) a rotation of the amide arms around the N(cycle)−C bound leading to a Δ−Λ configurational change; (2) an inversion of the cyclen cycle configuration (δδδδ-λλλλ). The enantiomerization can proceed either by successive or concerted occurrence of these two processes. Figure 4 summarizes these concepts in a visual manner. Previous studies of $[Ln(DOTA)(H_2O)]^-$ complexes using ^1H 2D-EXSY[22,23] or variable temperature ^{13}C NMR[6,8] showed that the arm rotation is faster than the ring inversion. The introduction of a substituent at the α position of the ring nitrogen drastically slows down the arm rotation, so that the ring inversion becomes faster.[24]

Magnetization transfer is the method of choice to unambiguously distinguish the exchange pathways involved in the isomerization processes of $[Eu(DOTAM)(H_2O)]^{3+}$ at a given temperature. For example, if an equatorial cycle proton (M_{eq2}) of M is selectively inverted, the effect can be observed on the same equatorial proton (m_{eq2}) of m (arm rotation), on an axial proton (m_{ax1}) of m (ring inversion) or on an axial proton (M_{ax1}) of M (enantiomerization) as shown in Figure 5a. The experiment was performed at 250 K on different signals using an I-Burp shaped pulse for the selective inversion (typical pulse duration and power: 12 ms, 45 dB). The evolution of the signal intensities were fitted to the Mc-Connell equations (Figure 5b).[25,26] The effect of the arm rotation is strong, and this process is the fastest (M → m: $k_a^{250} = 60 \pm 10$ s^{-1}; m → M: $k_a^{250} = 260 \pm 50$ s^{-1}). The effect of the ring inversion is very weak and could not be fitted; the effect of the enantiomerization is detected when it involves two signals of M: $k_e^{250} = 1 \pm 1$ s^{-1} which is a limiting lower value for the ring inversion. As expected from studies on $[Ln(DOTA)(H_2O)]^-$ complexes,[6,8,23] the arm rotation is the fastest process (see Figure 5). To have a visual description of these exchange processes, we performed a 2D-EXSY (using a classical NOESY pulse sequence with a short mixing time of 20 ms at 250 K). It clearly shows (Supporting Information, Figure S3) strong cross-peaks due to the arm rotation and only a very weak interaction due to the enantiomerization is observable; no cross-peak coming from ring inversion is observed. The arm rotation being much faster than the other processes, we can consider that it is the only exchange process contributing significantly to the line broadening.

Therefore we can use a variable temperature study of the ^1H NMR ligand line widths to calculate the activation parameters

(20) Aime, S.; Botta, M.; Fasano, M.; Marques, M. P. M.; Geraldes, C. F. G. C.; Pubanz, D.; Merbach, A. E. *Inorg. Chem.* **1997**, *36*, 2059−2068.
(21) Micskei, K.; Helm, L.; Brücher, E.; Merbach, A. E. *Inorg. Chem.* **1993**, *32*, 3844−3850.
(22) Hoeft, S.; Roth, K. *Chem. Ber.* **1993**, *126*, 869−873.
(23) Jacques, V.; Desreux, J. F. *Inorg. Chem.* **1994**, *33*, 4048−4053.
(24) Howard, J. A. K.; Kenwright, A. M.; Moloney, J. M.; Parker, D.; Port, M.; Navet, M.; Rousseau, O.; Woods, M. *J. Chem. Soc., Chem. Commun.* **1998**, 1381−1382.
(25) McConnell H. M. *J. Chem. Phys.* **1958**, *28*, 430−431.
(26) Led, J. J.; Gesmar, H. *J. Magn. Res.* **1982**, *49*, 444−463.

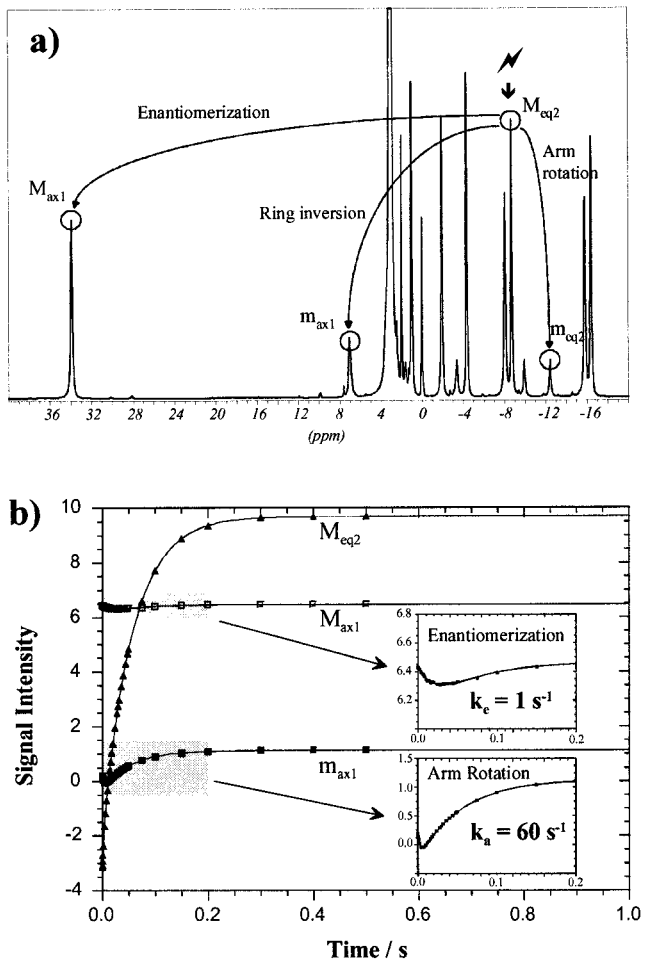

Figure 5. (a) ^{1}H NMR spectrum of $[Eu(DOTAM)(H_2O)]^{3+}$ ([Eu] = 10 mM, bound water/free water = 0.033) in CD_3CN at 252 K. The arrows show the possible pathways of the magnetization transfer resulting from the selective inversion of an equatorial cycle proton of the M-isomer (↓). (b) Evolution of the signal intensities as a function of time after selective inversion of M_{eq2}. The triangles stand for the M_{eq2} signal, the filled squares for the M_{ax1} signal and the unfilled squares for the m_{ax1} signal; the lines represent the evolution fitted to the McConnell equations.

of the interconversion (arm rotation). First we observed that the equilibrium constant $K = [M]/[m] = 4.5$ does not vary with the temperature, which is in good agreement with the small variation measured for $[Eu(DOTA)(H_2O)]^-$.[20] The temperature dependence of the measured line widths was fitted using exact solutions of the modified Bloch equations for a system in chemical exchange.[27] This yielded the following rate and activation parameters: M → m: $\Delta H^{\ddagger} = 39.1 \pm 1.9$ kJ mol^{-1}, $\Delta S^{\ddagger} = -52.1 \pm 7.4$ J K^{-1}mol^{-1}, $k^{250} = 68 \pm 5$ s^{-1} (Table 2); note that the interconversion rate at 250 K is the same as the one measured by magnetization transfer giving a good proof for our assumption that arm rotation is the only exchange process contributing significantly to the line broadening. The parameters for the m → M interconversion were calculated from the value for the M → m process considering the equilibrium constant $K = 4.5$.

A variable pressure study was performed at 256 K from 0.1 to 200 MPa. At this temperature the exchange contribution to the line width is between 80 and 90% depending on the observed signal. The activation volumes were calculated from the pressure dependence of the measured line widths (Figure 3) as described above (eq 1, 3, 5): M → m: $\Delta V^{\ddagger} = -0.5 \pm 0.3$ cm^3 mol^{-1}, m → M: $\Delta V^{\ddagger} = -0.5 \pm 0.7$ cm^3 mol^{-1}. Furthermore, the effect of pressure on a chemical equilibrium may be described by eq 6, where K_P is the equilibrium constant at pressure P, K_0 is the equilibrium constant at zero pressure, $\Delta V°$ is the reaction volume, R is the gas constant, and T is the temperature.

$$\ln(K_p) = \ln(K_0) - (\Delta V° P/RT) \qquad (6)$$

Thus, measuring the equilibrium constant K as a function of pressure allows the determination of $\Delta V°$. The measured reaction volume for the isomerization of $[Eu(DOTAM)(H_2O)]^{3+}$ is 0 ± 1 cm^3 mol^{-1} as expected for a process that only involves the rearrangement of the ligand around the metal center.

Correlation between Water Exchange and Interconversion. The NMR line widths of the bound water and of the ligand have similar behavior upon temperature changes, i.e., they have similar activation enthalpies (Table 2, and Supporting Information, Figure S4). This is particularly true if one takes into account the strong correlation between the activation enthalpies and entropies, which is not reflected in the associated statistical errors. Therefore, we fitted simultaneously the water exchange on M (eqs 1−3) and the interconversion (exact solutions of the modified Bloch equations, vide supra); using the same activation enthalpies, new kinetic parameters that fit very well the experimental data were obtained (Figure 6): $\Delta H^{\ddagger} = 45.7 \pm 1.4$ kJ mol^{-1}, water exchange rate on M: $k_{ex}^{250} = 180 \pm 20$ s^{-1}, M → m interconversion rate: $k^{250} = 57 \pm 4$ s^{-1}, the other parameters are given in Table 2. We observe that one M → m interconversion happens every two to three exchanges of a water molecule on M.

Our chemical intuition would suggest that the water must at least partially leave the inner-sphere to allow the arm rotation and hence the interconversion to take place. From this point of view, we can think of two limiting mechanisms:

(1) The activation enthalpies for the water exchange and the interconversion could be similar by accident; the two processes would then run independently with different pathways, the water exchange following a dissociatively interchange mechanism and the interconversion an interchange mechanism involving the rotation of the amide arms. In this scenario, both the water exchange and the interconversion start with the stretching of the bond between Eu(III) and the innersphere water, which explains the similar enthalpies of the two processes. An incoming water molecule leads then to the transition state of the water exchange, and independently the rotation of the arms leads to the transition state of the interconversion. In this case the interconversion does not require the exchange of the bound water molecule (See Figure S5 in Supporting Information).

(2) The similarity of the independent and simultaneous analysis of the water exchange and the interconversion could also be interpreted in terms of a common pathway for the two processes. We propose the energy and volume profiles depicted in Figure 7 where the two nonhydrated complexes M′ and m′ are intermediates in both the water exchange and the interconversion processes. This profile is in agreement with a dissociative mechanism for the water exchange on M ($\Delta V^{\ddagger} = 4.9 \pm 1$ cm^3 mol^{-1}) which is not rate limiting for an interchange activated interconversion ($\Delta V^{\ddagger} = -0.5 \pm 0.3$ cm^3 mol^{-1}). We would like to emphasize this mechanism as it clearly shows the necessity of a nonhydrated intermediate in the interconversion pathway, illustrating well our intuition that the interconversion depends on the water exchange.

(27) McLaughlin, A. C.; Leigh, J. S., Jr. *J. Magn. Res.* **1973**, *9*, 296−304.

Table 2. Kinetic and Activation Parameters for the Water Exchange on the M- and m-Isomers and for the M ⇄ m Interconversions Obtained from Independent and Simultaneous Fitting of the Variable Temperature and Pressure Data as well as by Magnetization Transfer

	independent fittings				simultaneous fittings		magnetization transfer
	water exchange [a]		interconversion [b]		water exchange	interconv.:	interconv.:
	on M	on m	M → m	m → M	on M	M → m	M → m
$k^{250}/10^3$ s^{-1}	0.11 ± 0.01	8.9 ± 0.6	0.068 ± 0.01	0.310 ± 0.01	0.18 ± 0.02	0.057 ± 0.004	0.060 ± 0.01
$k^{298}/10^3$ s^{-1}	8.3 ± 0.3	327 ± 60	1.7 ± 0.2	7.65 ± 0.2	7.6 ± 0.4	2.4 ± 0.2	
$\Delta H^{\ddagger}$/kJ mol^{-1}	53.1 ± 2	44.2 ± 2	39.1 ± 2		45.7 ± 1		
$\Delta S^{\ddagger}$/J K^{-1}mol^{-1}	+8.4 ± 5	+8.8 ± 7	−52.1 ± 7	−39.4 ± 7	−17.3 ± 5	−27.0 ± 5	
$\Delta V^{\ddagger}$/cm^3 mol^{-1}	4.9 ± 1		−0.5 ± 0.3	−0.5 ± 0.7			

[a] Simultaneous fit of ^{1}H and ^{17}O NMR transverse relaxation rates (see Table 1). [b] The parameters were obtained considering an equilibrium constant K = [M]/[m] = 4.5 independent of the temperature, i.e., the same activation enthalpy $\Delta H^{\ddagger}$.

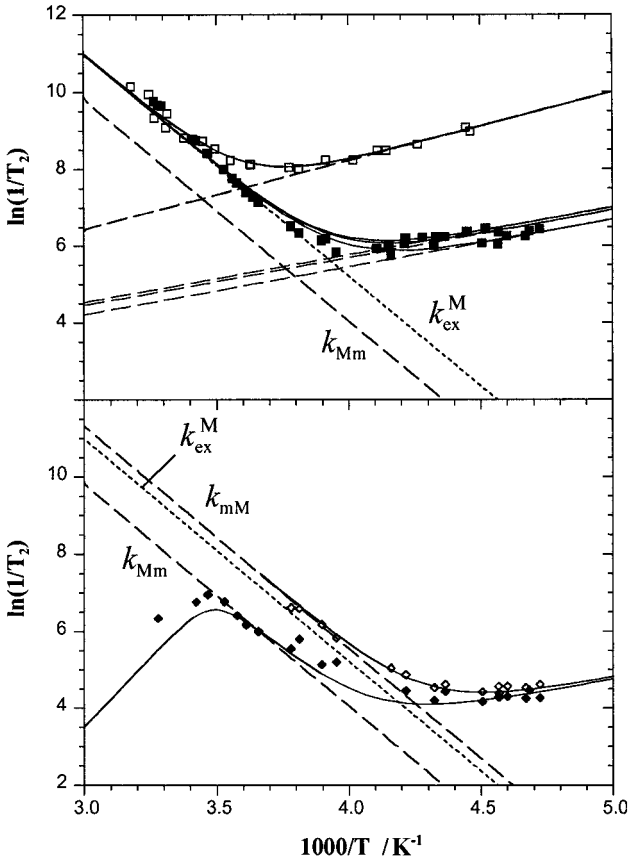

Figure 6. Simultaneous fit of the water exchange and the isomer interconversion considering the same activation enthalpy for both processes. Upper part: the filled and unfilled squares stand for the ^{1}H and the ^{17}O NMR data of the water bound to the M-isomer, respectively; the solid, dotted, and dashed lines stand for the fitted transverse relaxation rate, the exchange contribution, and the transverse relaxation rate without exchange, respectively; the calculated exchange rate of the M → m interconversion is represented with a dashed line and designed as k_{Mm}. Lower part: the filled and unfilled diamonds stand for the M_{eq2} and the m_{eq2} protons, respectively. The full lines represent the calculated transverse relaxation rates, the dashed lines the interconversion contribution to the transverse relaxation rate (k_{Mm} and k_{mM}), and the dotted line the water exchange rate on the M-isomer (k_{ex}^{M}).

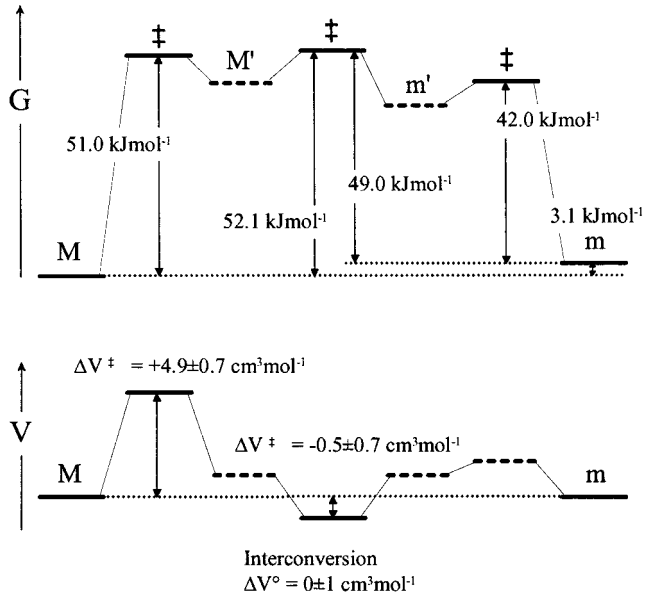

Figure 7. Energy and volume profiles for the M/m system, considering nonhydrated eight coordinated intermediates M′ and m′ in both the water exchange and the interconversion processes.

Conclusion

The first observation of the bound water signals on Eu(DOTA-like) complexes by ^{1}H and ^{17}O NMR allows the understanding of the water exchange individually for each isomer. Variable temperature and pressure NMR techniques give access to the activation parameters governing the water exchange and the interconversion processes and reveal how the interconversion depends on water exchange. At this stage further similar complexes should be studied before considering this as a general rule. Such a rule would be of primary importance for the design of fast water-exchanging Gd(III)-based contrast agents, as the M → m interconversion would always be slower than the water exchange on M. It shows the necessity to synthesize complexes which mainly exist in the fast exchanging m form in solution.

Acknowledgment. This work was financially supported by the Swiss National Science Foundation and the Swiss OFES as part of the European COST D8 action. We are grateful to Alessandro Barge for synthetic work, as well as Mauro Botta, Lothar Helm, and Éva Tóth for fruitful comments and discussions.

Supporting Information Available: Independent fits of the ^{1}H and ^{17}O NMR experimental data of the water exchange on the M-isomer (Figure S1). Simulation of the free water line width with the Swift and Connick approximation (Figure S2). 2D-EXSY ^{1}H NMR spectrum at 252 K (Figure S3). Comparison of the experimental data and separate fits of the water exchange on M and the M → m interconversion (Figure S4). Energy and volume profiles considering an dissociatively interchange mechanism for the water exchange and an independent interchange mechanism for the M → m interconversion (Figure S5). Composition of the studied solutions (Table S1). Experimental NMR data as follows: temperature dependence of the ^{1}H and ^{17}O NMR line widths and resonances of the water signals (Tables S2−S9); pressure dependence of the ^{1}H and ^{17}O NMR line widths of the water signals (Tables S10, S11); temperature

dependence of the ^{1}H NMR line widths of the M_{eq2}, m_{eq2}, M_{ax1}, and m_{ax1} ligand signals (Tables S12, S13) (see Figure 4, M ⇄ m interconversion chapter for an explanation of signal attribution); temperature dependence of the ^{1}H NMR chemical shift difference between the $M_{eq2}-m_{eq2}$ and $M_{ax1}-m_{ax1}$ ligand signals (Tables S14); pressure dependence of the ^{1}H NMR line widths of the M_{eq2} and m_{eq2} ligand signals (Tables S15). Signal intensities evolution in the magnetization transfer experiment after the selective inversion of the M_{eq2} signal (Table S16). This material is available free of charge via Internet at http://pubs.acs.org.

JA993204S